Short hydrogen-hydrogen separation in RNiInH$_{1.333}$ (R=La, Ce, Nd)

P. Vajeeston,[1,*] P. Ravindran,[1] R. Vidya,[1] A. Kjekshus,[1] H. Fjellvåg,[1,2] and V. A. Yartys[2]
[1]*Department of Chemistry, University of Oslo, Box 1033, Blindern, N-0315, Oslo, Norway*
[2]*Institute for Energy Technology, N-2027 Kjeller, Norway*

(Received 2 July 2002; revised manuscript received 19 September 2002; published 15 January 2003)

First-principle studies on the total energy, electronic structure, and bonding nature of RNiIn (R=La, Ce, and Nd), and their saturated hydrides ($R_3Ni_3In_3H_4$=RNiInH$_{1.333}$) are performed using a full-potential linear muffin-tin orbital approach. This series of phases crystallizes in a ZrNiAl-type structural frame-work. When hydrogen is introduced in the RNiIn matrix, anisotropic lattice expansion is observed along [001] and lattice contraction along [100]. In order to establish the equilibrium structural parameters for these compounds we have performed force minimization as well as volume and c/a optimization. The optimized atomic positions, cell volume, and c/a ratio are in very good agreement with recent experimental findings. From the electronic structure and charge density, charge difference, and electron localization function analyses the microscopic origin of the anisotropic change in lattice parameters on hydrogenation of RNiIn has been identified. The hydrides concerned, with their theoretically calculated interatomic H-H distances of ~1.57 Å, violate the ''2-Å rule'' for H-H separation in metal hydrides. The shortest internuclear Ni-H separation is almost equal to the sum of the covalent radii. H is bonded to Ni in an H-Ni-H dumbbell-shaped linear array, with a character of NiH_2 subunits. Density of states, valence charge density, charge transfer plot, and electron localization function analyses clearly indicate significant ionic bonding between Ni and H and weak metallic bonding between H-H. The paired and localized electron distribution at the H site is polarized toward La and In which reduces the repulsive interaction between negatively charged H atoms. This could explain the unusually short H-H separation in these materials. The calculations show that all these materials have a metallic character.

DOI: 10.1103/PhysRevB.67.014101 PACS number(s): 81.05.Je, 71.15.Nc, 71.20.−b

I. INTRODUCTION

Hydrogen is considered as an ideal fuel for many types of energy converters. However, neither storage of hydrogen as a compressed gas nor as a cryogenic liquid appears suitable and economical for most types of potential applications. In this respect hydrogen storage in the form of a metal hydride is a promising alternative with many attractive features.[1,2] Over the past few decades, a major challenge which still remains, is to identify optimal candidates in intermetallics for such hydrogen storage. Rare-earth (R) alloys seem promising, owing to a high hydrogen capacity per volume unit and an ability to absorb hydrogen under moderate conditions.[1,3] The hydrogen absorption properties of these alloys are very much dependent on the constituents, and metal-hydrogen bonding interactions play a major role in the stability of the hydrides. In order to optimize an intermetallic phase for a certain application, an improved understanding of the role of individual alloy constituents in relation to electronic and structural properties is desirable. Several empirical models[4] have been proposed for the heat of formation and heat of solid solution of metal hydrides, and attempts have been made to rationalize the maximum hydrogen absorption capacity of certain alloy matrices.[5–7] These models infer that the metal-hydrogen interaction depend both on geometric and electronic factors.

Numerous phases between transition metals and nonmetals can accommodate hydrogen in the form of solid-solution or stoichiometric hydride phases. The amount of hydrogen per unit volume in metal hydrides is very high; in fact in some cases higher than in liquid or solid dihydrogen, e.g., VH_2 stores more than twice the amount of solid dihydrogen at 4.2 K. It is unfortunate, however, that most metal hydrides are heavy in relation to the amount of hydrogen they contain. The crystal structures of these phases are often complex and there are several potential interstices that might accommodate the hydrogen depending on factors like the size and shape of the interstitial site, chemical nature of the surrounding atoms, and the distances to coordinating atoms and hydrogen neighbors.[8,9]

Structural studies of intermetallic hydrides have revealed empirical rules that can be used to predict features of the hydrogen sublattice in a given matrix.[10,11] The ''2-Å rule'' is one such guideline, which states that the H-H distance[11] in a metal hydride must exceed 2 Å, and there is also theoretical evidence[12] in support of this rule. The nonmetallic, complex hydride K_2ReH_9 (Refs. 13 and 14) appears to provide an example of violation of the rule, with an H-H separation of 1.87 Å, whereas recent experimental[15] and theoretical[16] results for Th_2AlH_4 agree on a closest H-H separation of around 1.95 Å.

The recent experimental findings for deuterides with the ZrNiAl-type structural matrix ($LaNiInD_{1.225}$, $CeNiInD_{1.236}$, and $NdNiInD_{1.192}$) prove that very short D-D distances of about 1.5–1.6 Å are indeed possible.[17] The reason for this behavior is not yet understood, but it is expected that more insight may provide new ideas for how hydrogen can be packed in an efficient way in an alloy matrix. Nuclear magnetic resonance (NMR) study on $CeNiInH_x$ (x=1 and 1.6) (Refs. 18 and 19) and $PrNiInH_{1.29}$ (Ref. 20) have given independent indications of H..H pairing in these phases [1.48 Å for the H-H distance in $CeNiInH_x$ (Ref. 18) and 1.5 to 1.8 Å in $PrNiInH_{1.29}$]. Recent powder neutron diffraction (PND) data suggested that the H-H interaction is mediated via triangular R_3 structural units, where strong R-R bonds prob-

ably "shield" the direct H-H interaction.[17] However, for the isostructural phase $LaNiInH_x$ there appears to be no evidence of hydrogen pairing.[21]

We have recently shown[22] the violation of 2-Å rule in $RTInH_{1.333}$ (where T=Ni, Pd, or Pt) and the present paper is the full account of electronic structure and bonding behavior in this class of metal hydrides. In this paper we present the results of accurate full-potential linear muffin-tin orbital calculations on RNiIn (R=La, Ce, and Nd) and RNiInH$_{1.333}$. The main scope of the study is to reproduce the experimentally observed short H-H separations and, if so, to understand the reasons behind this behavior. Also it is of interest to identify reasons for the anisotropic lattice expansion during hydrogenation of RNiIn.

Details about structural aspects and computational methods are described in Sec. II. Section III gives the results of the calculations and comparisons with experimental findings. The most important conclusions are briefly summarized in Sec. IV.

II. STRUCTURAL ASPECTS AND COMPUTATIONAL DETAILS

A. Structural features

ABC aluminides usually crystallize with the ZrNiAl-type structure.[23,24] On substituting Al with larger In atoms in *R*-based analogs, the *ab* plane of the hexagonal structure expands considerably relative to the *c* axis. This makes hydrogen absorption more favorable owing to enlarged interstitial sites. In RNiIn phases, both the $4h$ and $6i$ sites are candidates for hydrogen absorption.[18,19] Recent experimental results show that $4h$ site is fully occupied in $R_3Ni_3In_3H_4$ hydrides. In these saturated RNiInH$_{1.333}$ hydrides the H atoms are located inside R_3Ni tetrahedra that share a common face, thereby forming a R_3Ni_2 trigonal bipyramid.

Both the RNiIn intermetallic phases and the RNiInH$_{1.333}$ hydrides crystallize in a hexagonal ZrNiAl-type structure with space group $P\bar{6}2m$, structural details being summarized in Table I and illustrated in Fig. 1. The unit cell contains 13 atoms of which Ni occupies two different crystallographic sites, Ni($1b$) in the $1b$ position and Ni($2c$) in the $2c$ position.

B. Computational details

The theoretical approach is based on the generalized-gradient approximation with the Perdew *et al.*[25] proposed exchange correlation of density-functional theory. The Kohn-Sham equation was solved by means of a full-potential linear muffin-tin orbital method.[26] The calculations were relativistic including spin-orbit coupling and employed no shape approximation to the charge density and potential. Spin-orbit terms are included directly in the Hamiltonian matrix elements inside the muffin-tin spheres. The basis functions, charge density, and potential were expanded in spherical harmonic series inside the muffin-tin spheres and in Fourier series in the interstitial regions. The spherical-harmonic expansion of the charge density, potential, and basis functions were carried out up to $l = 6$. The tails of the basis functions

TABLE I. Optimized atomic coordinates for RNiIn and RNiInH$_{1.3333}$. Ni atoms occupy two different sets of atomic positions: Ni($1b$) in $1b$ at 0,0,1/2 and Ni($2c$) in $2c$ at 1/3,2/3,0 and 2/3,1/3,0.

	Theory			Experiment (Ref. 17)		
	x	y	z	x	y	z
LaNiIn						
La	0.5866	0	1/2	0.5940	0	1/2
In	0.2475	0	0	0.2560	0	0
$LaNiInH_{1.3333}$						
La	0.6036	0	1/2	0.6035	0	1/2
In	0.2444	0	0	0.2437	0	0
H	1/3	2/3	0.6728	1/3	2/3	0.6759
CeNiIn						
Ce	0.5880	0	1/2	0.5940	0	1/2
In	0.2480	0	0	0.2560	0	0
$CeNiInH_{1.3333}$						
Ce	0.6077	0	1/2	0.6013	0	1/2
In	0.2507	0	0	0.2462	0	0
H	1/3	2/3	0.6752	1/3	2/3	0.6737
NdNiIn						
Nd	0.5886	0	1/2	0.5940	0	1/2
In	0.2496	0	0	0.2560	0	0
$NdNiInH_{1.3333}$						
Nd	0.6013	0	1/2	0.6013	0	1/2
In	0.2483	0	0	0.2462	0	0
H	1/3	2/3	0.6723	1/3	2/3	0.6737

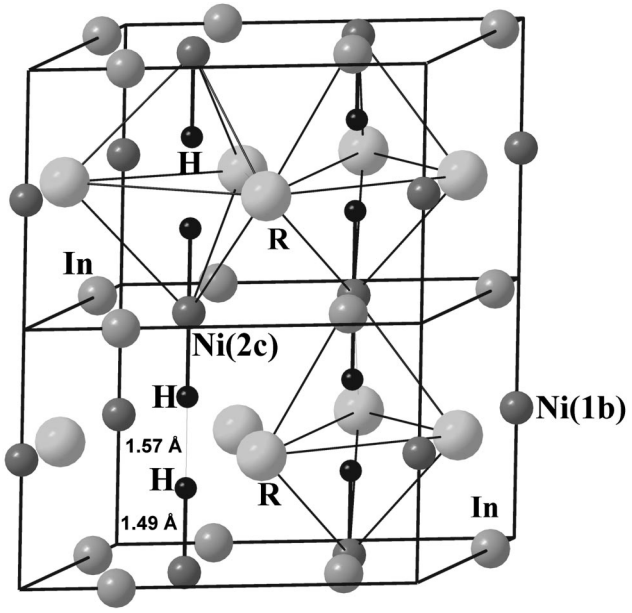

FIG. 1. The crystal structure of RNiInH$_{1.333}$(R=La, Ce, and Nd). Legends for the different kinds of atoms are given in the illustration. The linear H-Ni($2c$)-H array is marked with thicker connecting lines.

outside their parent spheres are linear combinations of Hankel or Neumann functions depending on the sign of the kinetic energy of the basis function in the interstitial regions. For the core-charge density, the Dirac equation is solved self-consistently, i.e., no frozen core approximation is used. Our calculations concern ideal and fully saturated hydrides with the composition $R_3Ni_3In_3H_4$ (RNiInH$_{1.333}$). The ratio of the interstitial to unit-cell volume is around 0.42. The basis set contained semicore $5p$ and valence $5d$, $6s$, $6p$, and $4f$ states for La [for Ce the $4f$ electrons are treated as valence and localized core electrons, whereas Nd-$4f$ electrons are treated as localized electrons using the open core approximation). In the open core approximation we treated the f electrons as localized and removed their contribution in the valence band. This is equivalent to the local density approximation (LDA)$+U$ approach with $U=\infty$ for the f electrons. A similar type of approach was successfully used in Ref. 27], $4s$, $4p$, and $3d$ states for Ni, $5s$, $5p$, and $5d$ states for In, and $1s$, $2p$, and $3d$ states for H. All orbitals were contained in the same energy panel. A so-called multibasis was included, to ensure a well-converged wave function, implying the use of different Hankel or Neuman functions each attaching to their radial functions. This is important in order to obtain a reliable description of the higher-lying unoccupied states and lower-lying semicore states. Integration over the Brillouin zone was done using ''special-point'' sampling,[28] and self consistency was obtained with 105 **k** points in the irreducible part of the Brillouin zone of the hexagonal Bravais lattice, which corresponds to 768 **k** points in the whole Brillouin zone. Test calculations were made for the double number of **k** points to check for convergence, but the optimized c/a ratio for 105 and 210 **k** points for LaNiInH$_{1.333}$ are essentially same. Hence 105 **k** points were used for the optimization of c/a, unit-cell volume, and atomic positions as well as the calculation of electron density. For the density of states (DOS) calculations, the Brillouin-zone integration was performed by means of the tetrahedron method.[29]

To gauge the bond strength we have used crystal orbital Hamiltonian population [COHP (Ref. 30)] analyses, as is implemented in the TBLMTO-47 package.[31,32] The COHP, which is the Hamiltonian population weighted density of states, is identical to the crystal orbital overlap population. If the COHP is negative, it indicates bonding character, whereas a positive COHP indicates antibonding character. The bulk moduli have been obtained using the so-called universal-equation-of-state fit for the total energy as a function of volume.

III. RESULTS AND DISCUSSION

Structural optimizations were carried out in order to understand the anisotropic expansion effect during incorporation of H in the RNiIn matrix and to verify the experimental H-H separation in RNiInH$_{1.333}$. Experimental structural information for the RNiIn phases was used as input. First, a relaxation of atomic positions globally using the force-minimization technique (forces are minimized up to 0.002 mRy/a.u.) was done, keeping the experimental c/a and unit-cell volume (V_0) fixed. Thereafter the theoretical equilibrium volume was determined by fixing the optimized atomic positions and the experimental c/a, while varying the unit-cell volume between -15% and 10% of V_0 (see Fig. 2). Next c/a was optimized by a $\pm 2\%$ variation of c/a (in steps of 0.02) while keeping the theoretical equilibrium unit-cell volume fixed (Fig. 3). The theoretically obtained structural parameters are presented along with experimental data in Tables I and II. The corresponding interatomic distances are tabulated in Table III. Finally, using the theoretically obtained structural parameters for the RNiIn phases as a starting point, hydrogen was inserted into the $4h$ site and the entire structural optimization procedure was repeated. Our optimized atomic positions (Table I) and lattice parameters (Table II) are in very good agreement with the recent PND results,[17] and the small differences found may partly be attributed to non-stoichiometry with respect to hydrogen which experimentally is of the order of 10%. Hence the calculations confirm the unusual shortest H-H separation in RNiInH$_{1.333}$. We also find that the volume expansion (LaNiIn: 2.54 Å^3/H, CeNiIn: 4.45 Å^3/H and NdNiIn: 3.93 Å^3/H) on hydrogenation is highly anisotropic, with a large lattice expansion along [001] ($\Delta c/c = 12.7$–16.7%) and a small lattice contraction along [100] ($-\Delta a/a = 1.7$–4.0%). The results presented in the rest of the paper are

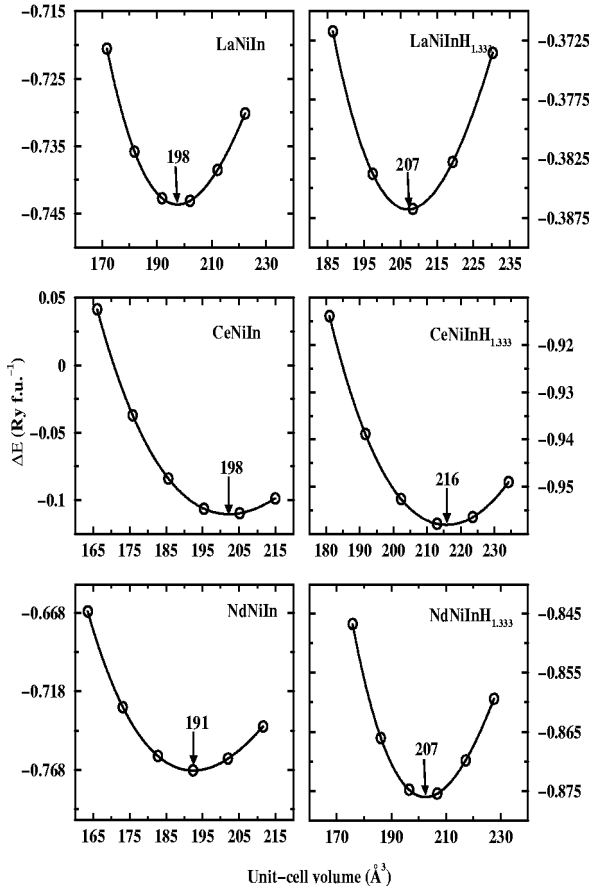

FIG. 2. Total-energy curves for RNiIn and RNiInH$_{1.333}$ as functions of V/V_0. LaNiIn ($E=-31\,803+\Delta E$), LaNiInH$_{1.333}$ ($E=-31\,805+\Delta E$), CeNiIn ($E=-32\,539+\Delta E$), CeNiInH$_{1.333}$ ($E=-32\,540+\Delta E$), NdNiIn ($E=-34\,068+\Delta E$), and NdNiInH$_{1.333}$ ($E=-34\,069+\Delta E$).

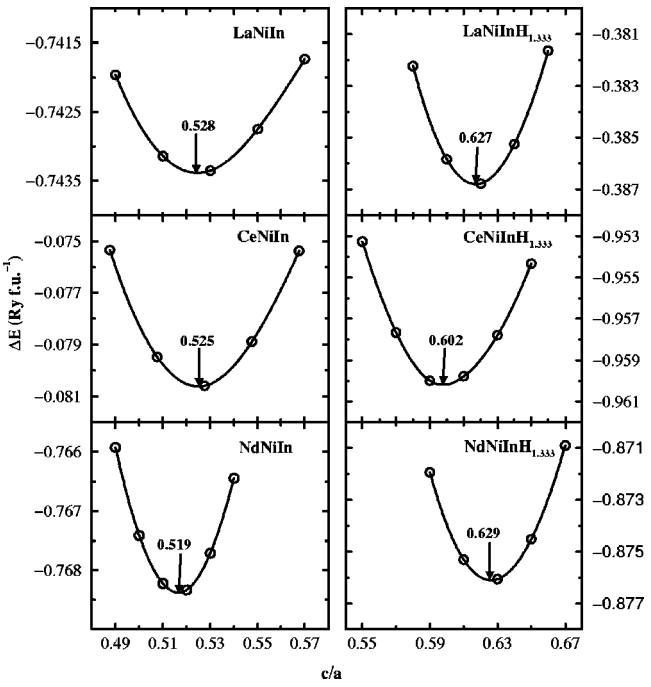

FIG. 3. Total-energy curves for RNiIn and RNiInH$_{1.333}$ as a function of c/a. (Also see the caption to Fig. 2).

based on the theoretical equilibrium lattice parameters.

CeNiIn is a valence-fluctuating system with Kondo-like behavior.[33] Hydrogenation of the isoelectronic CeNiAl phase[34,35] [like CeNiAlH$_{2.04}$ (Ref. 36)] induces a localization of the Ce-4f electrons. In order to establish the valence of Ce in CeNiIn and CeNiInH$_{1.333}$, we have made total energy calculations as a function of cell volume (see Fig. 4) for different electronic configurations [e.g., a trivalent state with 4f electrons as valence electrons (designated $4f^1$ valence), one 4f electron as localized in the core state (designated $4f^1$ localized) and two 4f electrons as localized in the core state (designated $4f^2$ localized)] using constrained density-functional calculations. From the minima in the total-energy curves (see Fig. 4) we have obtained the equilibrium unit-cell volumes for Ce in different electronic configurations for CeNiInH$_{1.333}$: 238.48 Å^3 for $4f^2$ localized, 215.89 Å^3 for $4f^1$ localized, and 194.02 Å^3 for $4f^1$ valence. The $4f^1$-localized value 215.89 Å fits very well with an experimental unit-cell volume of 212.93 Å^3, indicating that Ce exists as Ce^{3+} with one 4f electron well localized in CeNiInH$_{1.333}$ (similarly for CeN:In).

Using the universal-equation-of-state fit[37] for the total energy as a function of the unit-cell volume, the bulk modulus (B_0) and its pressure derivative (B_0') are obtained (Table II). B_0 for LaNiIn and CeNiIn decreases on hydrogenation, which can be explained as a consequence of the volume-expansion during hydrogenation. In the case of NdNiIn B_0 increases on hydrogenation, indicating that the introduction of hydrogen in the NdNiIn lattice enhances the bond strength such that it overcomes the volume expansion effect. There are no experimental bulk moduli available for these materials.

A. Ni-H and H-H separation

Compared to binary metal-hydride structures which are characterized by a few relatively simple and usually highly symmetrical configurations, ternary metal-hydride structures show a great variety of complex and often low-symmetric configurations. In the latter class hydrides, one may find metal-hydrogen distances close to the sum of the covalent radii concerned (e.g., for β'-MgNiH$_4$ the experimental Ni-H distance is 1.49 Å, as compared with the sum of the covalent radii 1.47 Å).

In the RNiInH$_{1.333}$ phases the hydrogen 4h site is fully occupied and all H atoms have the same environment in the crystal lattice. The Ni(2c)-H distance is 1.457–1.493 Å depending on R (see Table III) which matches the sum of covalent radii for Ni and H. This may be associated with the H-Ni-H (NiH$_2$-molecule-like) subunits which occur in these structures. Another interesting feature of these structures is the short H-H separations. Such situations may occur when the two H atoms concerned form an occupied H-H bonding state with the empty anti-bonding states[38] above the Fermi level (E_F). The thus resulting structural H$_2$ "dimers" located inside the alloy matrix may give rise to highly unusual

TABLE II. Calculated lattice parameters (in Å), c/a, variation in a ($\Delta a/a$), c ($\Delta c/c$), and volume ($\Delta V/V$) on hydrogenation (in %), density of states at the Fermi level [$N(E_F)$ in states Ry^{-1} f.u.$^{-1}$], bulk modulus (B_0 in GPa) and its pressure derivative(B_0') for RNiIn and RNiInH$_{1.333}$.

	LaNiIn		LaNiInH$_{1.333}$		CeNiIn		CeNiInH$_{1.333}$		NdNiIn		NdNiInH$_{1.333}$	
	Theor.	Expt. (Ref. 17)	Theor.	Expt. (Ref. 17)	Theor.	Expt. (Ref. 17)	Theor.	Expt. (Ref. 17)	Theor.	Expt. (Ref. 17)	Theor.	Expt. (Ref. 17)
a	7.5604	7.5906	7.2603	7.3810	7.5807	7.5340	7.4536	7.2921	7.5207	7.5202	7.2408	7.2255
c	3.9924	4.0500	4.5522	4.6489	3.9806	3.9750	4.4871	4.6238	3.9023	3.9278	4.5560	4.5752
c/a	0.5281	0.5336	0.6270	0.6399	0.5251	0.5276	0.6020	0.6341	0.5189	0.5223	0.6292	0.6332
$\Delta a/a$	—	—	−3.97	−2.76	—	—	−1.68	−3.21	—	—	−3.72	−3.92
$\Delta c/c$	—	—	14.02	14.8	—	—	12.72	16.3	—	—	16.75	16.50
$\Delta V/V$	—	—	5.15	8.54	—	—	8.97	8.98	—	—	7.60	7.53
$N(E_F)$	38.22	—	35.30	—	38.90	—	38.10	—	43.74	—	28.13	—
B_0	70.38	—	69.45	—	86.24	—	81.67	—	76.20	—	86.03	—
B_0'	4.12	—	4.08	—	2.88	—	3.48	—	4.35	—	4.12	—

TABLE III. Interatomic distances (in Å) and ICOHP (in eV) for RNiIn and RNiInH$_{1.333}$.

	RNiIn			RNiInH$_{1.333}$		
	Theor.	Expt. (Ref. 17)	ICOHP	Theor.	Expt. (Ref. 17)	ICOHP
R=La						
Ni($2c$)-H	—	—	—	1.4891	1.5065	−3.44
H-H	—	—	—	1.5734	1.6350	−0.14
La-H	—	—	—	2.3609	2.4064	−0.72
Ni($2c$)-In	2.8993	2.8688	−1.26	2.7990	2.8490	−0.85
La-Ni($1b$)	3.1251	3.0359	−0.67	2.8791	2.9262	−0.86
Ni($1b$)-In	2.7358	2.8062	−1.24	2.8857	2.9390	−1.21
Ni($2c$)-La	3.0290	3.0783	−0.66	3.1835	3.2441	−0.61
R=Ce						
Ni($2c$)-H	—	—	—	1.4573	1.5086	−3.32
H-H	—	—	—	1.5721	1.6061	−0.22
Ce-H	—	—	—	2.4271	2.3708	−0.79
Ni($2c$)-In	2.9045	2.8474	−1.22	2.8427	2.8026	−0.87
Ce-Ni($1b$)	3.1229	3.0133	−0.54	2.9237	2.9070	−0.88
Ni($1b$)-In	2.7375	2.7692	−1.19	2.9192	2.9268	−1.33
Ni($2c$)-Ce	3.0320	3.0407	−0.57	3.2102	3.2124	−0.63
R=Nd						
Ni($2c$)-H	—	—	—	1.4928	1.5064	−3.34
H-H	—	—	—	1.5699	1.5618	−0.23
Nd-H	—	—	—	2.3499	2.3421	−0.69
Ni($2c$)-In	2.7667	2.7308	−1.14	2.7731	2.7704	−0.84
Nd-Ni($1b$)	2.9785	2.9331	−0.25	2.8866	2.8870	−0.65
Ni($1b$)-In	2.9075	2.9415	−1.21	2.9015	2.9038	−1.35
Ni($2c$)-Nd	3.1572	3.1690	−0.39	3.1771	3.1793	−0.64

behaviors.[39] This could have been the case for the RNiInH$_{1.333}$ phases where the experimental findings as well as our structural optimization study show H-H separations of around 1.57 Å. However, a detailed theoretical analysis (see below) reveals quite a different type of bonding situation between the H atoms.

B. Electronic structure

In general a hydrogen atom modifies the electronic structure of a host alloy by the creation of metal-hydrogen bonding states, a shift of the Fermi level, a change in the width of bands, and/or a modification of the lattice symmetry. The calculated band structures for LaNiIn and LaNiInH$_{1.333}$ are shown in Fig. 5. These illustrations clearly indicate that the insertion of H in the LaNiIn matrix has a noticeable impact on the band structure, mainly in the valence-band (VB) region. Three low-lying bands [see Fig. 5(a) where a single s band and a doubly degenerated p-band are seen at the Γ point] originate mainly from In-5s and Ni-4s electrons. Hybridized In-5p, Ni-3d, and La-5d bands are present in an energy range from −3 to −1 eV, and the electrons corresponding to these bands are mainly participating in the chemical bonding. Similar band structures are obtained for CeNiIn, NdNiIn, and their hydrides (not shown). The unoccupied La-4f states are found in the conduction-band region around 2.5 eV above E_F. As the unit cell contains three formula units, four electrons are additionally introduced when LaNiInH$_{1.333}$ is formed from LaNiIn. Therefore two additional s bands are present in the lower part of the VB (from −8.5 to −3 eV) in LaNiInH$_{1.333}$. The lowest-energy band in Fig. 5(b) near the Γ point (behaves almost like a free-electron band) corresponds to one of these H-1s bands. The other H-1s band is well dispersed and hybridized with the rest of the VB in the region from around −6 to −3 eV. A cluster of well-localized bands in the VB around −2 eV originates from the Ni-3d electrons. Owing to the introduction of extra electrons in the lowest portion of the VB, the hybridized bands are moved toward E_F by the addition of hydrogen. As seen from Fig. 5 several bands cross E_F, and hence these phases will exhibit metallic behavior. This is further confirmed by the total DOS profiles which show a finite number of electrons at the Fermi level.

C. Nature of chemical bonding

Insight into the nature of the chemical bonding may provide a clearer picture of the reasons for the short Ni-H and H-H separations in these phases. In order to identify the type of bonding and to gain more knowledge we have analyzed the DOS, charge density, electron localization function (ELF), and COHP characteristics.

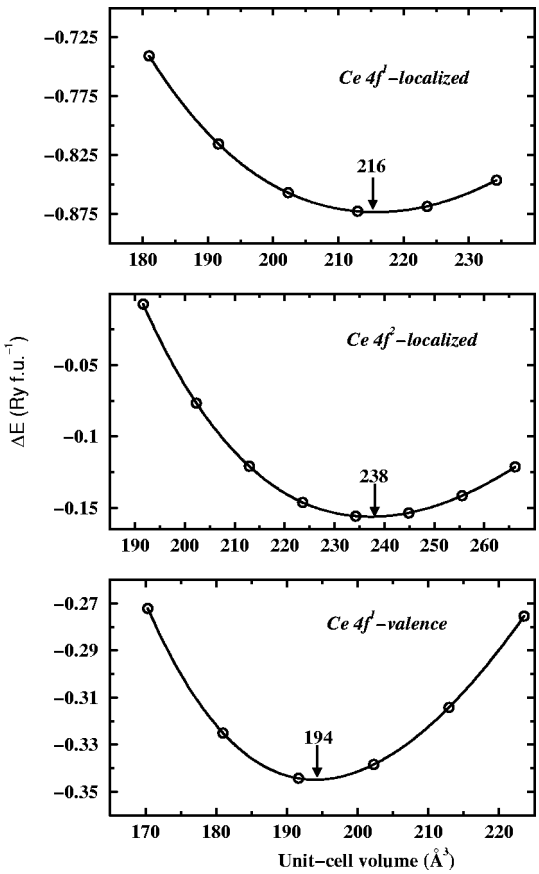

FIG. 4. Total energy vs V/V_0 for $CeNiInH_{1.333}$, with different possible valence states for Ce. The experimental volume from diffraction studies is $V_0 = 212.93$ Å^3 (Ref. 17).

1. DOS

All the DOS curves for *R*NiIn and *R*$NiInH_{1.333}$ show close similarities (Fig. 6). A striking feature of Fig. 6 is that the hydrogenated phases have a pseudogap, i.e., a deep valley closer to E_F, most pronounced for $CeNiInH_{1.333}$. The strong Ni($2c$)-H interaction is mainly responsible for this pseudogap. In general, a gain in total energy can be obtained when E_F lies in the vicinity of a pseudogap.[40] On moving from La to Nd, the additional *f* electrons are treated as localized electrons that do not participate in the chemical bonding. However, due to the variation in the interatomic distances, there are small differences in the broadening of the DOS. The metallic character of all these phases mainly origi-

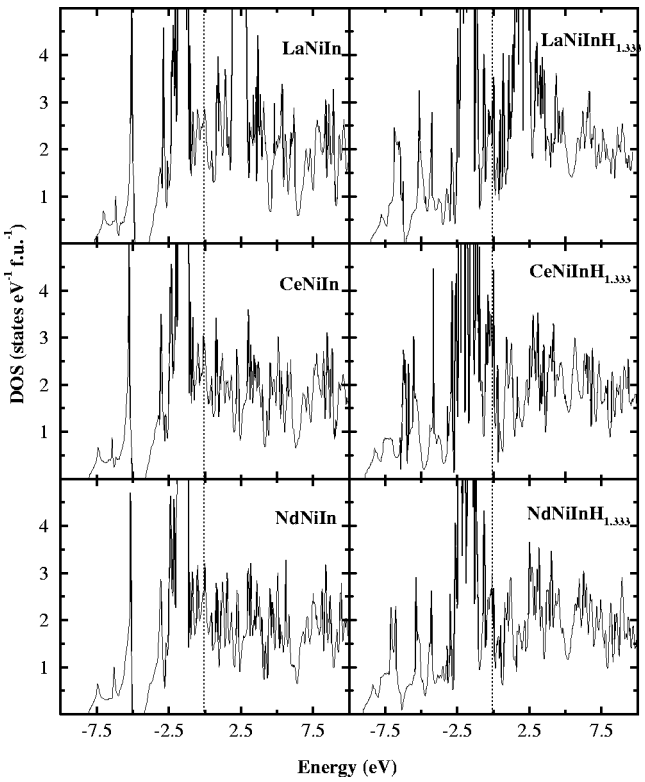

FIG. 6. Total DOS for *R*NiIn and *R*$NiInH_{1.333}$ (*R* = La, Ce, Nd).

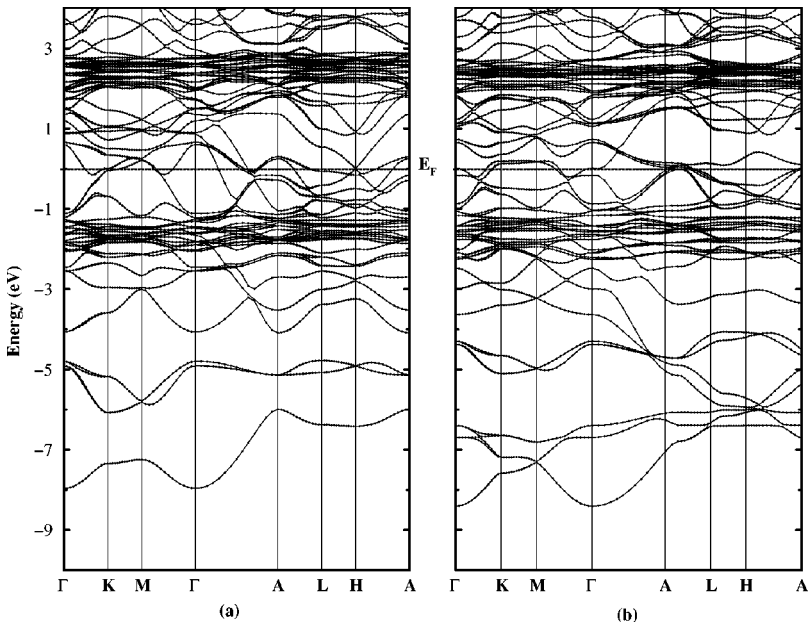

FIG. 5. Energy bands $[E(k)]$ for (a) LaNiIn and (b) $LaNiInH_{1.333}$. High-symmetry directions in the Brillouin zone are marked. The Fermi energy is set to zero.

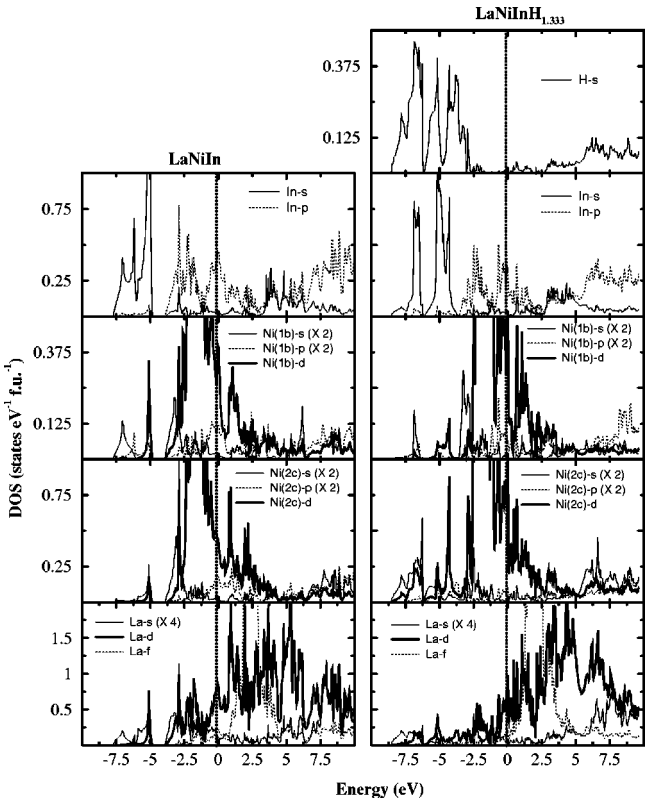

FIG. 7. Site- and orbital-projected DOS's for LaNiIn and $LaNiInH_{1.333}$.

nates from the finite contributions to the DOS at E_F from R-5d, Ni-3d, and In-5p states.

The calculated partial density of states (PDOS) (Ref. 41) is a useful tool to analyze the nature of the chemical bonding in solids. In order to follow the changes in electronic structure on hydrogenation, Fig. 7 displays the calculated PDOS for LaNiIn and $LaNiInH_{1.333}$. In the lower portion of the PDOS curve for LaNiIn there occurs a gap (from ~ -5 to -4.2 eV), below which In-s and Ni-s states are present. The energy range -4.2 eV to E_F carries a large number of electronic states with mainly La-5d, Ni-3d, and In-5p characters. These states are energetically degenerate, which implies that it is possible to form covalent Ni(1b)-R, Ni(2c)-R, R-In, Ni(1b)-In, and Ni(2c)-In bonds. The interatomic Ni(1b)-In and Ni(2c)-In distances are much shorter than Ni(2c)-R (Table III). Hence the formation of covalent bonding between Ni(1b) or Ni(2c) and In is favorable both from energetical and spatial points of view. The unoccupied states are dominated by La-4f contributions, in particular above ~ 1 eV.

When H is introduced into the RNiIn matrix the atoms are somewhat rearranged (see Tables I and III) in order to accommodate the hydrogens, and the energy levels are modified accordingly. NMR studies[21] on $LaNiInH_x$ showed that $N(E_F)$ does not vary appreciably with the H content. The calculated $N(E_F)$ values for LaNiIn and $LaNiInH_{1.333}$ are not significantly different, and this observation is consistent with the NMR findings. In CeNiIn also $N(E_F)$ does not change considerably upon hydrogenation. In contrast, $N(E_F)$ for

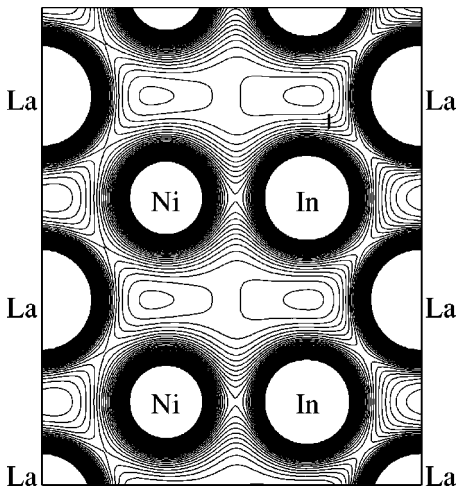

FIG. 8. Valence-electron-density plot for LaNiIn in the (100) plane [the origin being shifted to (0.303,0.198, 0.315)]. 25 contours between 0 and 0.075 electrons/a.u.^{3}. Ni refers to Ni(2c).

NdNiIn is drastically decreased upon hydrogenation (see Table II). One common feature of the electronic structure of these hydrides is the occurrence of H states at the bottom of the VB. The inclusion of the additional H-s states in the energy range from -8 to -3 eV changed not only this portion of the DOS, but also systematically shifted the E_F toward the unoccupied states in the unhydrogenated phases. Moreover the energy gap between -5 and -4.2 eV disappears on going from the alloy matrix to the corresponding hydride. Another interesting consequence for the DOS upon hydrogenation is that In-s states become broadened as a result of the reduced interatomic distance between Ni(2c) and In (i.e., following the lattice contraction along a). H-s, In-s, Ni-d, and La-p states are energetically degenerate in an energy range from -8.2 to -3.4 eV in $LaNiInH_{1.333}$, implying a possible covalent bonding contribution for the combinations In-H, Ni-H, La-H, and H-H. Since the Ni(2c)-H separation is very short this combination becomes more favorable for covalent bonding than the others. However, more Ni(2c)-d electrons are accumulated near E_F; on the other hand, H-s states are well localized in the bottom of the VB, as a result possibility to form ionic bonding between Ni(2c) and H is more probable than covalent.

By the addition of hydrogen into the LaNiIn matrix the DOS's of Ni(1b) and Ni(2c) are both considerably broadened in an energy range from -8 to -4 eV. This is mainly due to the Ni(2c)-H interaction in the latter case and the reduction in the Ni(1b)-La distance in the former. However, the changes in DOS for Ni(2c) are more extensive than those for Ni(1b) by hydrogen addition, which is mainly due to the reduction in the Ni(2c)-In distance apart from the Ni(2c)-H interaction.

2. Charge density analysis

In order to understand the microscopic origin of the short Ni(2c)-H and H-H separations we have made valence charge density analyses in different crystal planes for the alloy matrix as well as the hydrogenated phases. Figures 8

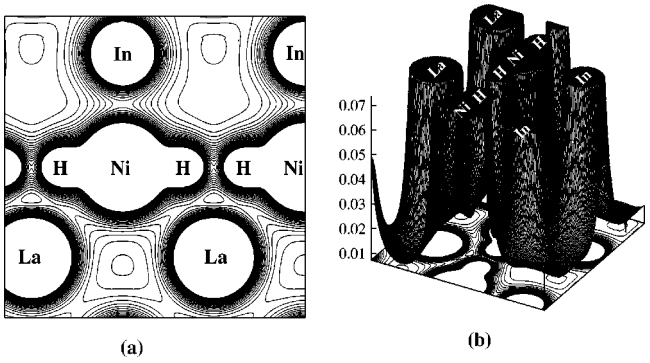

FIG. 9. Valence-electron-density plot for $LaNiInH_{1.333}$ in the (100) plane [the origin being shifted to (1/3,0,0)]. 25 contours between 0 and 0.075 electrons/a.u.^{3}. Ni refers to Ni($2c$).

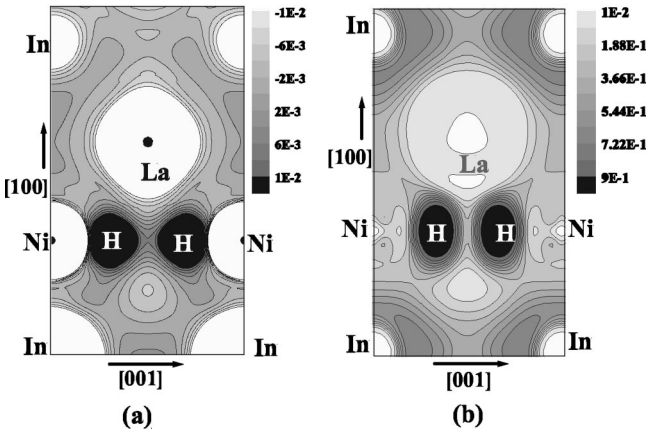

FIG. 10. (a) Charge transfer and (b) electron localization function plot for $LaNiInH_{1.333}$ in the (100) plane [origin is shifted to (1/3,0,0)].

and 9 show the (100) plane for LaNiIn and $LaNiInH_{1.333}$, respectively. Similar results were obtained for the analogous Ce and Nd phases.

The electronegativity difference between Ni and In is only 0.1, which indicates that covalent interaction between these atoms is more probable than ionic interaction. This is indeed confirmed by the charge density analysis (Fig. 8), which shows that there is finite electron density present between Ni($2c$) and In. In fact, as will be argued later, the Ni($2c$)-In bond is stronger than the other interatomic bonds in *R*NiIn. Ni($1b$)-*R* and In-*R* have a mixed (partial covalent, partial ionic) character which may be attributed to the electronegativity difference of 0.5 between *R* and Ni as well as between *R* and In. Alternating Ni($2c$) and In layers (see Fig. 8) have no charge accumulated between them indicating a interstitial void for potential accommodation of hydrogen.

When hydrogenation takes place the interstitial site is shifted (a small lattice contraction along a) toward Ni($2c$) (see Tables I and II) and a Ni($2c$)-H bond is formed. Ni($2c$) and H form a dumbbell-like linear arrangement along [001] which results in an appreciable lattice expansion along c. This rationalizes the anisotropic changes in the lattice. Another noteworthy finding is that the interatomic distance between Ni($2c$) and H is almost equal to the sum of the covalent radii of Ni and H, which gives the H-Ni($2c$)-H arrangement a distinct character of a linear NiH_2 molecule-like structural subunits (see Fig. 9). The same type of bonding is present in Na_2PdH_2,[42] and the Pd-H separation here (1.68 Å) is close to the Ni($2c$)-H separation in $RNiInH_{1.333}$, (1.46–1.49 Å), whereas the H-H separation in Na_2PdH_2 (3.35 Å) is much larger than in $RNiInH_{1.333}$ (1.570–1.573 Å).

The covalent bond strength of Ni($2c$)-In is reduced upon hydrogenation in spite of the reduction in the interatomic distance from 2.89 to 2.79 Å (see Sec. III C 4). This may be rationalized as another consequence of the formation of the NiH_2 structural unit which takes up some Ni($2c$)-3d electrons and prevent them from participating in the covalent bonding between Ni($2c$) and In. Although the H-H separation is very short, their mutual interaction is weak since very little electronic charge is present between them [see Fig. 9(b)]. The main reason for this behavior is again the NiH_2 structural subunit, which strongly involves the H-1s electron in the bonding to Ni($2c$). Hence an insufficient amount of electronic charge is left for repulsion between the hydrogen atoms which consequently can approach each other rather closely.

Our spin-polarized calculations for LaNiIn and $LaNiInH_{1.333}$ show that these systems always converge into a nonmagnetic state, implying a nonmagnetic ground state. We know that valence electrons participate either in bonding or in magnetism. As in this case Ni($2c$) and Ni($1b$) electrons participate in the bonding, a quenching of the magnetic moment results. However, in the Nd and Ce systems one may expect finite magnetic moments from localized 4f electrons. But we have not considered this magnetic aspect in our calculations.

3. Charge transfer and ELF analysis

To depict the role of the charge-transfer effect we have displayed the charge-transfer plot for $LaNiInH_{1.333}$ in (100) in Fig. 10(a). The charge-density transfer contour is the self-consistent electron density of the solid in a particular plane, minus the electron density of the free atoms in overlapping regions. This enables one to observe how the electrons are redistributed in a particular plane in the real crystal (compared to the free atoms) due to the bonding between them. From Fig. 10(a) it is clearly seen that electrons are transferred from La, In, and Ni to H, resulting in ionic bonding between H and the host lattice.

The ELF is another useful tool to distinguish different bonding interaction in solids.[43,44] The value of the ELF is limited to the range 0 to 1. High value of the ELF corresponds to a low Pauli kinetic energy, as can be found in covalent bonds or lone electron pairs. The ELF for $LaNiInH_{1.333}$ in (100) is displayed in Fig. 10(b). The large value of the ELF at the H site indicates strongly paired electrons. In between Ni($2c$) and H, delocalized metallic Ni($2c$)-d electrons are distributed; hence the ELF is low. Due to the repulsive interaction between H's, the ELF contours are not spherically shaped, but polarized toward La and In sites, which can explain why these materials have unusual short H-H separation (i.e., the polarization of electrons at the

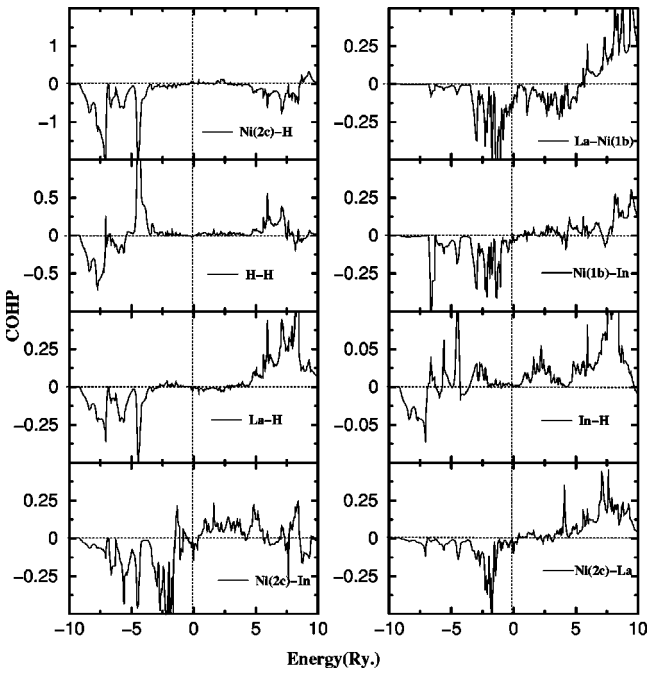

FIG. 11. COHPs for $LaNiInH_{1.333}$; referring to the short distances corresponding to the combinations Ni($2c$)-H, H-H, La-H, Ni($2c$)-In, Ni($1b$)-La, Ni($1b$)-In, In-H, and Ni($2c$)-La.

H site toward La and In give less electrons to participate in the repulsive interaction between the H atoms). The ELF value between Ni and In is 0.7; a typical value for covalent bonding, consistent with the conclusion arrived at from our charge-density analysis. A finite ELF (0.345) is present between H-H bonds, which indicates that the interaction between the H-H bonds is weak metallic.

4. COHP

A simple way to investigate the bond strength between two interacting atoms in a solid is to look at the complete COHP between them, taking all valence orbitals into account. In order to understand the bonding pattern further, results from such COHP analyses for $LaNiInH_{1.333}$ are shown in Fig. 11 for all possible interactions within a 3.5-Å range. This illustration shows that VB comprises mainly bonding orbitals (negative COHP) and that antibonding orbitals are found some ~ 3 eV above E_F. Integrated COHP (ICOHP) values up to E_F are included in Table III for all phases studied. The most notable feature being the remarkable strength of the Ni($2c$)-H interaction (-3.32 to -3.44 eV in ICOHP) compared with the other bonds.

As measured by ICOHP, the bonding interaction Ni($2c$)-In is reduced upon hydrogenation (from around -1.20 to -0.85 eV). The bonding ICOHP values for the short H-H separations are very small, around -0.04 eV (not listed in Table III, thus supporting the already advanced inference that there is no significant covalent bonding interaction between the H atoms (see Sec. III C 2). The low ICOHP value reflects the fact that both bonding and antibonding states are present below E_F, but even if one takes into account only the bonding states, ICOHP remains low [-0.14 to -0.23 eV, which is much smaller than ICOHP for Ni($2c$)-H]. Hence both COHP and charge-density analyses agree that the H-H interaction is considerably weaker than the Ni($2c$)-H interaction. Our conclusion therefore disagrees with NMR findings for $CeNiInH_x$ and $PrNiInH_x$,[18–20] which concluded that H..H pairing is the main reason for the unusually short H-H separation in these hydrides. On the basis of the PND results[17] it has been speculated that the H-H interaction is shielded by R-R interaction. However, our COHP study shows that the R-R interaction is only from -0.61 to -0.62 eV in ICOHP (not included in Fig. 11) which is 5–6 times smaller than for the Ni($2c$)-H interaction and closer to the bond strength for R-H and R-Ni($2c$).

The experimental and theoretical studies show highly anisotropic lattice expansion on hydrogenation of RNiIn. Now let us try to understand the reason for this anisotropic lattice expansion. According to the crystal structure of RNiIn, the possible positions for hydrogen accommodation are $6i$ and $4h$ sites. However, from a hole size point of view the $4h$ site is more favorable than the $6i$ site (the hole size for the $4h$ site is ca. 0.4 Å, whereas that for the $6i$ site is less than 0.34 Å). The optimized atom position of hydrogenated compounds show that the structural deformation does not lead to any substantial rearrangement of metal atoms in the basal plane. None of the atoms are significantly shifted in x and y coordinates from those of the intermetallic RNiIn. This may be because all atoms are bonded strongly (from the COHP study) in the ab plane; hence there is no room for H in the Ni($2c$),In plane. When H occupies a $4h$ site the atoms try to rearrange themselves to have a minimum energy configuration. Hence the only possibility to expand the lattice is along the [001] direction. Our charge-density study clearly indicates the formation of Ni-H-Ni linear chains along [001], implying an expansion along the c axis. The charge-transfer plot shows that during the formation of a hydride phase, some charges transfer from the electron-rich metal atoms to the H site. This may lead to a contraction in the ab plane, hence resulting in anisotropic lattice changes upon hydrogenation.

5. H-H interaction

In order to elucidate the present findings further we made the following model calculations. First we fixed all structural variables, except those for the H position at their theoretically derived equilibrium values. Then we changed the H-H separation (moving the hydrogen atoms either toward or away from each other, i.e., we allowed H to move in the z direction alone, keeping x and y parameters fixed), and calculated the total energy as a function of the H-H separation. Such a H displacement is equivalent to a shortening or enlargement of the Ni($2c$)-H distance depending upon the actual shift of the hydrogen. A shortening of the H-H distance corresponds to a decrease in the Ni($2c$)-H interaction and an increase in the repulsive interaction between H atoms. The thus obtained total energy as a function of H displacement is

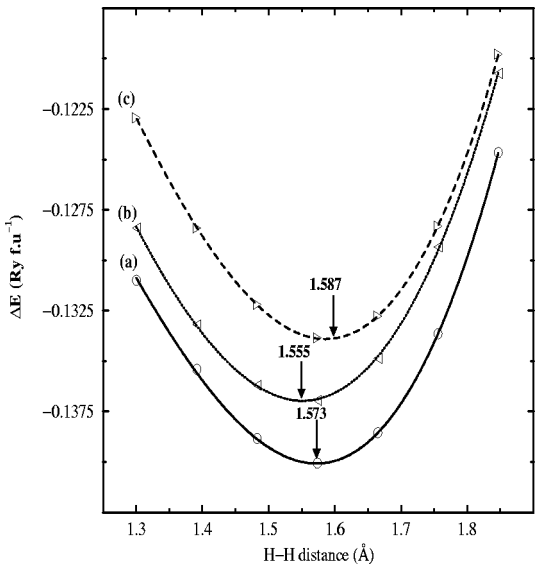

FIG. 12. Total energy vs H-H distance in $LaNiInH_{1.333}$ ($E=-31805+\Delta E$). (a) All atoms, except H, are fixed at their equilibrium positions. (b) La atoms are moved 0.05 Å out of their equilibrium position toward H. (c) La atoms are moved 0.05 Å out of their equilibrium position away from H.

shown in Fig. 12(a). The minimum in the total energy corresponds to the equilibrium H-H separation obtained by the structural optimization procedure.

In order to consider the shielding mechanism suggested in Ref. 17, we have made two sets of additional model calculations. The total energy has been calculated as a function of the H-H separation, keeping Ni and In fixed in their equilibrium positions, by either [Fig. 12(b)] moving La 0.05 Å out of its equilibrium position toward H or [Fig. 12(c)] moving La 0.05 Å out of its equilibrium position away from H. The lowest total energy is obtained when all atoms, except H, are kept at their equilibrium positions [Fig. 12(a)]. The equilibrium H-H separations are 1.573, 1.555, and 1.587 Å, for the three models in Fig. 12(a), (b), and (c), respectively.

Let us now try to understand the variation in total energy with H-H separation in these compounds. A shortening of the H-H separation corresponds to a reduction in the Ni($2c$)-H interaction and an enhanced repulsive interaction between the H atoms. As the total energy curves increase steadily upon a shortening of the H-H separations, the possibility of stabilizing hydrogen in the form of molecular H_2-like units seems to be completely ruled out. The total energy also increases drastically for increasing H-H separations beyond the equilibrium value. This is due to a decrease in the covalent H-H interaction and the increasing repulsive Ni($2c$)-H interaction. The considerable changes in the equilibrium H-H distance on R displacement indicate that R in the bipyramidal configuration (see Fig. 1) acts as a shielding, and to some extent compensates for the repulsive H-H interaction. Calculations show that when the R-H separation is reduced the H atoms are allowed to come closer to each other.

It would be interesting to study whether the short H-H separation is due to special aspects of the ZrNiAl-type crystal structure or whether strong Ni($2c$)-H interactions can also be generalized to other intermetallics. In order to test this hypothesis and furthermore to identify potential hydrides with short H-H separations we are currently considering the effect on the H-H separation by replacement of Ni by other metals. The results will be published in a forthcoming paper.

IV. CONCLUSION

We have carried out investigations of the electronic structure and bonding in RNiIn and RNiInH$_{1.333}$ (R=La, Ce or Nd, with a ZrNiAl-type basic framework) using generalized-gradient-corrected full-potential density-functional calculations, and have arrived at the following conclusions.

(1) The optimized lattice constants exhibit a highly anisotropic lattice expansion (13–17 %) along [001] and a small contraction (-1.7 to -4.0%) along [100] upon hydrogenation of RNiIn, in very good agreement with experimental findings. The optimized atomic coordinates, unit-cell volumes, and c/a ratios are in very good agreement with experimental findings.

(2) All these compounds violate the so-called ''2-Å rule'' for metal hydrides. RNiInH$_{1.333}$ is found to have the shortest H-H separation hitherto reported for hydrogenated alloys.

(3) Charge-density and ELF studies show a weak metallic type of interaction between the hydrogen atoms. A charge-transfer plot clearly indicates that electrons are transferred from La, In, and Ni to H. Hence a strong ionic bonding is present between H and the host lattice. The short distances between H atoms in such metal hydrides are governed primarily by the polarization of negative charges on H toward the electropositive La and In.

(4) Model calculations show that H-H interaction is strongly repulsive, which makes an explanation based on formation of H_2 molecular subunits in the structure highly improbable. Considerable changes in the equilibrium H-H distance upon R displacement indicate that R in the bipyramidal configuration acts as a shielding and to some extent compensates for the repulsive H-H interaction.

(5) RNiIn and RNiInH$_{1.333}$ have a finite number of electrons at E_F, and are accordingly classified as metals.

ACKNOWLEDGMENTS

The authors gratefully acknowledge Professor John Wills and Professor O.K. Andersen for allowing to use their computer codes and Professor Andreas Savin and Dr. Florent Boucher for useful communications on ELF and COHP, respectively. P.V. and P.R. also acknowledge the Research Council of Norway for financial support and the grant of computing time on Norwegian supercomputers. P.R. wishes to thank Professor Olle Eriksson, Dr. Per Andersen, and Dr. Hakan Hugosson for useful communications.

*Electronic address: ponniahv@kjemi.uio.no; URL: http://www.folk.uio.no/ponniahv

[1] K. H. J. Buschow, H. H. Van Mall, P. D. Googwell, and P. S. Rudman, J. Less-Common Met. **29**, 203 (1972).
[2] J. J. Reilly and R. H. Wiswall, Inorg. Chem. **13**, 218 (1974).
[3] J. H. N. Van Vucht, F. A. Kuijpers, and H. C. M. Bruning, Philips Res. Rep. **25**, 133 (1970).
[4] A. R. Miedema, J. Less-Common Met. **32**, 117 (1973); A. R. Miedema, R. Boom, and F. R. de Boer, *ibid.* **41**, 283 (1975); P. E. P. Boutenand and A. R. Miedema, *ibid.* **71**, 147 (1980).
[5] D. G. Westlake, J. Less-Common Met. **103**, 203 (1984); **91**, 1 (1983).
[6] A. J. Maeland, A. F. Andersen, and K. Videm, J. Less-Common Met. **45**, 347 (1976); A. J. Maeland, L. E. Tanner, and G. G. Libowitz, *ibid.* **74**, 279 (1980).
[7] M. W. Mallet and I. E. Campell, J. Am. Chem. Soc. **73**, 4850 (1951); D. T. Peterson and J. Rexer, J. Less-Common Met. **4**, 95 (1962).
[8] K. Yvon, J. Less-Common Met. **103**, 53 (1991).
[9] S. Rundqvist, R. Tellgren, and Y. Anderson, J. Less-Common Met. **101**, 145 (1984).
[10] D. P. Shoemaker and C. B. Shoemaker, J. Less-Common Met. **68**, 43 (1979).
[11] C. Switendick, Z. Phys. Chem. B **117**, 89 (1979).
[12] B. K. Rao and P. Jena, Phys. Rev. B **31**, 6726 (1985).
[13] K. Yvon and P. Fischer, in *Hydrogen in Intermetallic Compounds*, edited by L. Schlapbach, Topics in Applied Physics Vol. 63 (Springer, Berlin, 1988), p. 87.
[14] S. C. Abrahams, A. P. Ginsberg, and K. Knox, Inorg. Chem. **3**, 558 (1964); K. Knox and A. P. Ginsberg, *ibid.* **3**, 555 (19641964)
[15] M. H. Sørby, H. Fjellvåg, B. C. Hauback, A. J. Maeland, and V. A. Yartys, J. Alloys Compd. **309**, 154 (2000).
[16] P. Vajeeston, R. Vidya, P. Ravindran, H. Fjellvåg, A. Kjekshus, and A. Skjeltorp, Phys. Rev. B **65**, 075101 (2002).
[17] V. A. Yartys, R. V. Denys, B. C. Hauback, H. Fjellvåg, I. I. Bulyk, A. B. Riabov, and Ya. M. Kalychak, J. Alloys Compd. **330-332**, 132 (2002).
[18] K. Ghoshray, B. Bandyopadhyay, M. Sen, A. Ghoshray, and N. Chatterjee, Phys. Rev. B **47**, 8277 (1993).
[19] M. Sen, S. Giri, K. Ghoshray, G. Bandyopadhyay, G. Ghoshray, and N. Chatterjee, Solid State Commun. **89**, 327 (1994).
[20] M. Sen, A. Ghoshray, K. Ghoshray, S. Sil, and N. Chatterjee, Phys. Rev. B **53**, 14345 (1996).
[21] M. Sen, K. Ghoshray, B. Bandyopadhyay, A. Ghoshray, and N. Chatterjee, Indian J. Phys. **69A**, 99 (1995).
[22] P. Ravindran, P. Vajeeston, R. Vidya, A. Kjekshus, and H. Fjellvåg, Phys. Rev. Lett. **89**, 106403 (2002).
[23] E. I. Hladyshevskiy and O. I. Bodak, *Crystal Chemistry of Intermetallic Compounds of Rare Earth Metals* (Vyscha Shkola, Lviv, 1982).
[24] I. I. Bulyk, V. A. Yartys, R. V. Denys, Ya. M. Kalychak, and I. R. Harris, J. Less-Common Met. **284**, 256 (1999).
[25] J. P. Perdew, in *Electronic Structure of Solids*, edited by P. Ziesche and H. Eschrig (Akademie Verlag, Berlin, 1991), p. 11; J.P. Perdew, K. Burke, and Y. Wang, Phys. Rev. B **54**, 16533 (1996); J. P. Perdew, K. Burke, and M. Ernzerhof, Phys. Rev. Lett. **77**, 3865 (1996).
[26] J. M. Wills and B. R. Cooper, Phys. Rev. B **36**, 3809 (1987); D. L. Price and B. R. Cooper, *ibid.* **39**, 4945 (1989).
[27] M. Richter, J. Phys. D **31**, 1017 (1998); C. Ambosch-Draxl, P. Blaha, and K. Schwarz, J. Phys.: Condens. Matter **6**, 2347 (1994); M. Divis, K. Schwarz, P. Blaha, G. Hilscher, H. Michor, and S. Khmelevskyi, Phys. Rev. B **62**, 6774 (2000); http://www.wien2k.at/reg_user/faq/open_core.html.
[28] D. J. Chaidi and M. L. Cohen, Phys. Rev. B **8**, 5747 (1973); S. Froyen, *ibid.* **39**, 3168 (1989).
[29] P. E. Blochl, O. Jepsen, and O. K. Andersen, Phys. Rev. B **49**, 16223 (1994).
[30] R. Dronskowski and P. E. Blochl, J. Phys. Chem. **97**, 8617 (1993).
[31] O. K. Andersen, Phys. Rev. B **12**, 3060 (1975); O. K. Andersen and O. Jepsen, Phys. Rev. Lett. **53**, 2571 (1984); H. L. Skriver, *The LMTO Method* (Springer, Heidelberg, 1984).
[32] G. Krier, O. Jepsen, A. Burkhardt, and O. K. Andersen, *Tight Binding LMTO-ASA Program Version 4.7* (Stuttgart, Germany, 2000).
[33] H. Fujii, T. Inoue, Y. Andoh, T. Takabatake, K. Satoh, Y. Maeno, T. Fujita, J. Sakurai, and Y. Yamaguchi, Phys. Rev. B **39**, 6840 (1989).
[34] L. Menon, A. Agarwal, and S. K. Malik, Physica B **230**, 201 (1983).
[35] Y. N. Grin, K. Hiebl, and P. Rogl, J. Less-Common Met. **110**, 299 (1985).
[36] B. Bandyopadhyay, K. Ghoshray, A. Ghoshray, and N. Chatterjee, Phys. Rev. B **38**, 8455 (1988).
[37] P. Vinet, J. H. Rose, J. Ferrante, and J. R. Smith, J. Phys.: Condens. Matter **1**, 1941 (1989).
[38] J. F. Halet, J. Y. Saillard, C. Koudou, C. Minot, Z. Nomikou, R. Hoffman, and C. Demangeat, Chem. Mater. **4**, 153 (1992).
[39] A. J. Maeland, in *Recent Advances in Hydride Chemistry*, edited by R. Poli (Elsevier, Amsterdam, 2001), p. 531.
[40] P. Ravindran and R. Asokamani, Bull. Mater. Sci. **20**, 613 (1997); P. Ravindran and R. Asokamani, Phys. Rev. B **50**, 668 (1994); J. H. Xu and A. J. Freeman, Phys. Rev. B **41**, 12553 (1990).
[41] C. D. Gelatt, A. R. Williams, and V. L. Moruzzi, Phys. Rev. B **27**, 2005 (1983).
[42] D. Noreus, K. W. Tonroos, A. Borje, T. Szabo, W. Bronger, H. Spittank, G. Auffermann, and P. Muller, J. Less-Common Met. **139**, 233 (1988).
[43] A. D. Becke and K. E. Edgecombe, J. Chem. Phys. **92**, 5397 (1990).
[44] A. Savin, A. D. Becke, J. Flad, R. Nesper, H. Preuss, and H. G. von Schnering, Angew. Chem. Int. Ed. Engl. **30**, 409 (1991); A. Savin, O. Jepsen, J. Flad, O. K. Andersen, H. Preuss, and H. G. von Schnering, *ibid.* **31**, 187 (1992).